

A Well Test Model for Composite Reservoir with Resistance Force on Interface

Sun He-Dong^{*a,b}, Liu Yue-wu^a and Shi Ying^c

^aMechanics, Chinese Academy of Sciences, Beijing, 100190, China; ^bLangfang Branch, Research Institute of Exploration and Development, Langfang, 065007, China; ^cResearch Institute of Exploration and Development, Tarim Petrochina, Kuerle, 834000, China

Abstract: Tazhong No.1 gas field is a typical vug-fractured carbonate gas condensate reservoir with the characteristics of high heterogeneity and complex geological and dynamics. A physical and effective hole-diameter mathematical model for well test in the composite reservoir is established, which considers the resistance force on interface. Specifically, the following factors are involved, including wellbore storage and skin factor of inner boundary, fracture open of interface, and infinite boundary of outer boundary. Moreover, the exact solution of wellbore pressure is obtained in terms of ordinary Bessel functions in the Laplace space. The numerical computation of the solution is obtained by using the Stehfest numerical inversion method, and the behavior of the system is studied as a function of various interface parameters. Results show that the composite radius controls the time of the interface performance. The larger the composite radius, the later the interface performance begins. In addition, the condition of open fracture has a heavy impact on the transitional zone performance. Resistance force on the interface disguises the influence of the condition of the open fracture, which is more apparent with larger resistance force. Comparisons with the regular well test model shows that the new model can improve the data utilization, reduce multiple solutions of well test analysis and increase the accuracy on the identification of formation parameters and evaluation stimulation. The method is useful for the reservoir dynamic description.

Keywords: Well test analysis model, resistance force on interface, open fracture, composite reservoir, Laplace transform.

1. INTRODUCTION

Tazhong 1 gas field is the largest carbonate platform margin reefal gas field in China, which is one of the most important fields of production expansion and reserve growth in Tarim basin [1, 2]. This gas field is with the characteristics of complex reservoirs, including cave type, fracture-cavity type, and fracture type. Besides, cave and tight carbonate matrix appear in the space randomly and alternatively with strong heterogeneity [3-5]. From the perspective of production performance, composite characteristic with supply has been shown in [6]. In addition, the obvious pressure difference is shown in the inner and outer regions. That is, after a period of production time, the energy is transferred from the outer region to the inner region. Existing studies show that filtration resistance exists in the interface between the inner region and the outer region. Specially, the influence of such resistance becomes more obvious in the case of low permeability than that of high permeability [7, 8]. There are essential differences between such pressure behavior and that with threshold pressure gradient [9, 10]. Although well test models have been constructed for composite reserves with the resistance force on the interface, such as homogeneous reservoir [8, 11, 12], double porosity reservoir [13] and triple porosity reservoir [14], the case with fracture open has not been

considered. Moreover, existing study is still in the stage of theoretical analysis while real case study has not been carried out.

In this study, a new well test model is constructed for the infinite composite reserves of natural fracture open in the interface. In addition, the type curve is drawn, and the corresponding dynamic characteristic is analyzed.

2. WELL TEST MODEL

2.1. Physical Model

The physical model of composite reserve proposed in this paper is shown in Fig. (1). To begin with, a few assumptions are given below:

- (1) The isotropic formation can be divided into 2 concentric regions. The inner zone, with a radius of r_1 and being the nearest to the wellbore, could contain a zone with the permeability reduced by drilling and improved permeability due to stimulation. The outer zone is the infinite reservoir. Each region is assumed to be uniform, and their reservoir and fluid properties are different from each other. The permeability, porosity, viscosity and total compressibility of the inner and outer zones are K_1 and K_2 , Φ_1 and Φ_2 , μ_1 and μ_2 , C_{11} and C_{12} , respectively.
- (2) Horizontal formation is with constant thickness, h .
- (3) Flow of a single phase fluid happens in either zone of the composite porous medium. Gravitational forces and

*Address correspondence to this author at the Mechanics, Chinese Academy of Sciences, Beijing 100190, China; Tel: 010-69213176; E-mail: sunhed@petrochina.com.cn

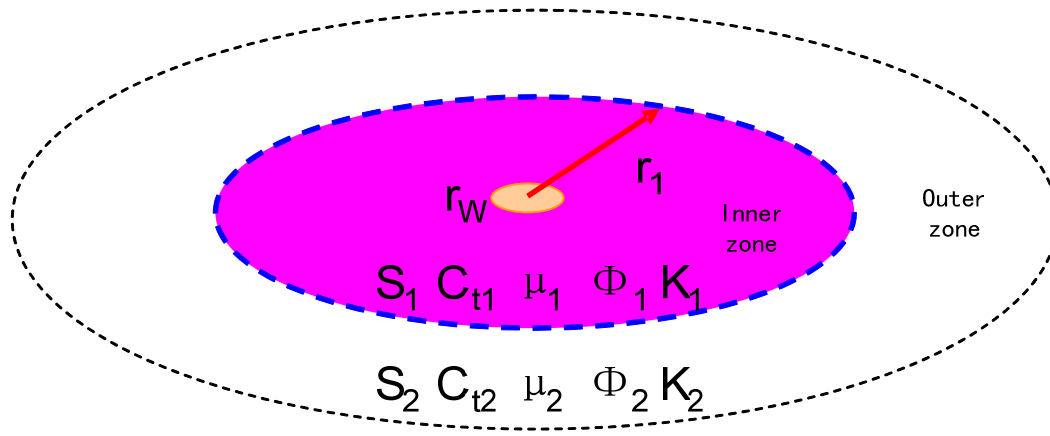


Fig. (1). Schematic of a two-region composite reservoir.

capillary force are negligible. Fluid flow obeys the Darcy law.

- (4) Well producing is at a constant rate from the center of the reservoir, and the skin effect is taken into consideration with a skin factor of S_1 . Wellbore storage factor is C .
- (5) The width of buttering between the inner zone and the outer zone is neglected, flow resistance force on buttering is concentrated on the interface of the two zones, which is represented by the skin factor S_2 , and the pressure jump happens when the flow goes through the interface.
- (6) During the production time t_p , the pressure difference between the two zones is larger than p_p , and the outer zone is involved with the flow.

2.2. Mathematical Model

In order to increase the stability of numerical calculation, the effective wellbore radius is inducted:

$$r_{we} = r_w e^{-S_1}$$

The mathematical model of the effective wellbore radius of the above physical problem is expressed by dimensionless variable as follows:

Control equation:

$$\frac{\partial^2 p_{1D}}{\partial r_D^2} + \frac{1}{r_D} \frac{\partial p_{1D}}{\partial r_D} - \frac{1}{C_D e^{2S_1}} \frac{\partial p_{1D}}{\partial (t_D/C_D)} = 0 \tag{1}$$

$$\frac{\partial^2 p_{2D}}{\partial r_D^2} + \frac{1}{r_D} \frac{\partial p_{2D}}{\partial r_D} - \frac{D_i}{C_D e^{2S_1}} \frac{\partial p_{2D}}{\partial (t_{2D}/C_D)} = 0 \quad t_{2D} = (t_D - t_{pD}) \tag{2}$$

Inner boundary condition:

$$p_{wD} = p_{1D} \tag{3}$$

$$\left(\frac{\partial p_{1D}}{\partial r_D} \right)_{r_D=1} = -1 + \frac{\partial p_{wD}}{\partial (t_D/C_D)} \tag{4}$$

Interface condition:

$$\left(\frac{\partial p_{1D}}{\partial r_D} \right)_{r_D=r_{1D}} = 0 \quad (t_D - t_{pD}) < 0 \tag{5}$$

$$p_{1D}(r_{1D}, t_D) = p_{2D}(r_{1D}, t_{2D}) + p_{pD} \quad (t_D - t_{pD}) = 0 \tag{6}$$

$$p_{1D}(r_{1D}, t_D) = p_{2D}(r_{1D}, t_{2D}) - S_2 \left(r_D \frac{\partial p_{2D}}{\partial r_D} \right)_{r_D=r_{1D}} \quad (t_D - t_{pD}) > 0 \tag{7}$$

$$\left(\frac{\partial p_{1D}}{\partial r_D} \right)_{r_D=r_{1D}} = \frac{1}{M} \left(\frac{\partial p_{2D}}{\partial r_D} \right)_{r_D=r_{1D}} \quad (t_D - t_{pD}) > 0 \tag{8}$$

Outer boundary condition:

$$p_{2D}(r_D \rightarrow \infty, t_{2D}) = 0 \tag{9}$$

Initial condition:

$$p_{1D}(r_D, 0) = p_{2D}(r_D, 0) = 0 \tag{10}$$

The dimensionless variables involved in the above mathematical model are defined as follows:

Dimensionless pressure $p_{jD} = \frac{2\pi(Kh)(p_0 - p_j)}{q\mu B} \quad j = 1, 2, p$;

Dimensionless time $t_D = \left(\frac{K}{\phi\mu C_t} \right) \frac{t}{r_w^2}$;

Dimensionless wellbore storage $C_D = \frac{C}{2\pi r_w^2} \left(\frac{1}{\phi h C_t} \right)_1$;

Mobility ratio $M = \frac{(K/\mu)_1}{(K/\mu)_2}$;

Storage capacity ratio $D_i = \frac{(K/\phi\mu C_t)_1}{(K/\phi\mu C_t)_2}$;

Dimensionless radius $r_D = r/r_w e^{-S_1}$;

Dimensionless radius of inner region $r_{1D} = r_1/r_w e^{-S_1}$;

Dimensionless time of outer region begin flow $t_{2D} = t_D - t_{pD}$

2.3. Solve the Mathematical Model

According to the Laplace transformation, the following equations are derived from equations (1) to (10). Equation (1) and (2) are expressed by Laplace variance z and s in Laplace space, respectively.

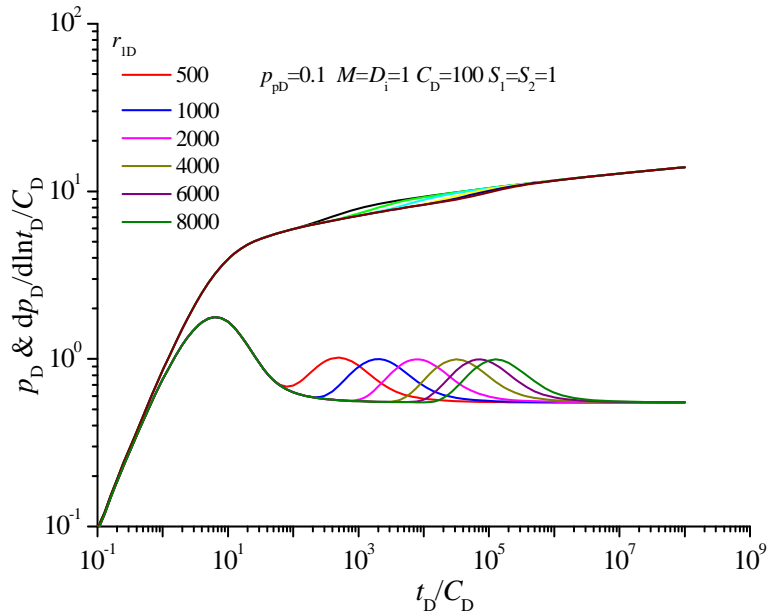


Fig. (2). The effect of dimensionless composite radius to type curve.

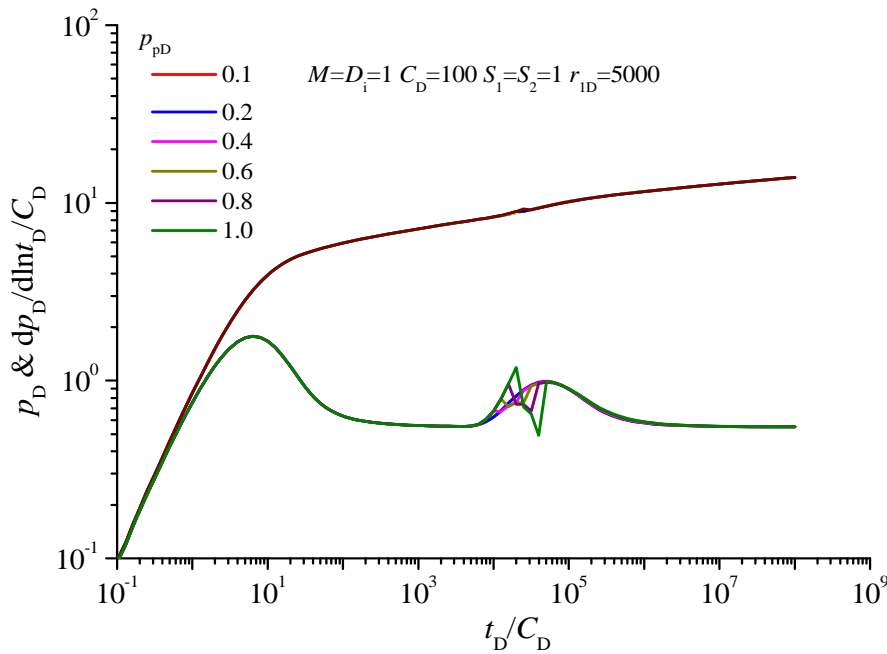


Fig. (3). The effect of dimensionless breakout pressure difference to type curve.

$$\frac{\partial^2 \bar{p}_{1D}}{\partial r_D^2} + \frac{1}{r_D} \frac{\partial \bar{p}_{1D}}{\partial r_D} - \frac{z}{C_D e^{2S_1}} \bar{p}_{1D} = 0 \tag{11}$$

$$\frac{\partial^2 \bar{p}_{2D}}{\partial r_D^2} + \frac{1}{r_D} \frac{\partial \bar{p}_{2D}}{\partial r_D} - \frac{sD_i}{C_D e^{2S_1}} \bar{p}_{2D} = 0 \tag{12}$$

2.3.1. Mathematical Model Solution – First Stage

The mathematical model of the first stage is composed of equations (1), (3), (4), (5) and (10). The bottomhole pressure in the Laplace space is:

$$\bar{p}_{wD}(1,z) = \frac{1}{z} \frac{\frac{K_1(r_{1D}\sqrt{\sigma_1})}{I_1(r_{1D}\sqrt{\sigma_1})} + \frac{K_0(\sqrt{\sigma_1})}{I_0(\sqrt{\sigma_1})}}{\frac{K_1(r_{1D}\sqrt{\sigma_1})}{I_1(r_{1D}\sqrt{\sigma_1})} \left[z - \sqrt{\sigma_1} \frac{I_1(\sqrt{\sigma_1})}{I_0(\sqrt{\sigma_1})} \right] + \left[z \frac{K_0(\sqrt{\sigma_1})}{I_0(\sqrt{\sigma_1})} + \sqrt{\sigma_1} \frac{K_1(\sqrt{\sigma_1})}{I_0(\sqrt{\sigma_1})} \right]} \tag{13}$$

Where

$$\sigma_1 = \frac{z}{C_D e^{2S_1}}$$

The pressure at the inner boundary is

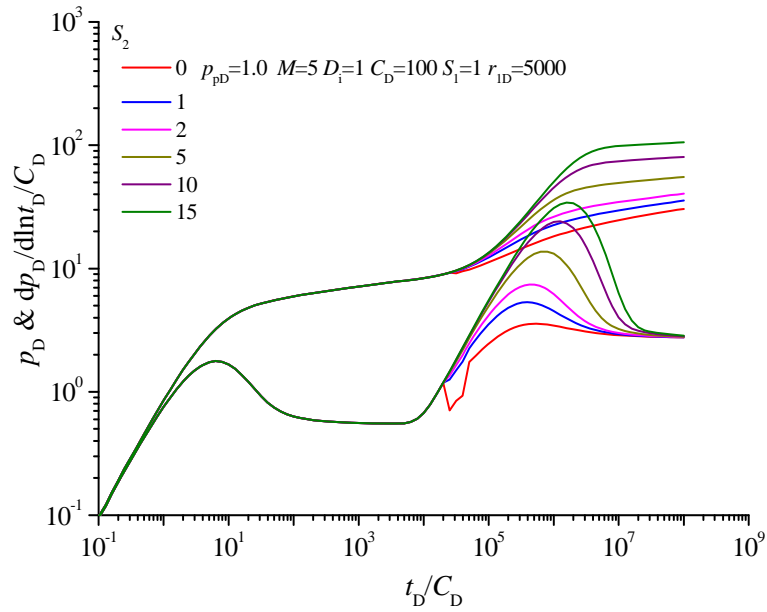


Fig. (4). The effect of interface additional resistance to type curve.

$$\bar{p}_{ID}(r_{ID}, z) = \frac{1}{z} \frac{\frac{K_1(r_{ID}\sqrt{\sigma_1}) + K_0(r_{ID}\sqrt{\sigma_1})}{I_1(r_{ID}\sqrt{\sigma_1}) + I_0(r_{ID}\sqrt{\sigma_1})}}{\frac{K_1(r_{ID}\sqrt{\sigma_1})}{I_1(r_{ID}\sqrt{\sigma_1})} + \frac{K_0(r_{ID}\sqrt{\sigma_1})}{I_0(r_{ID}\sqrt{\sigma_1})}} + \frac{zK_0(\sqrt{\sigma_1}) + \sqrt{\sigma_1}K_1(\sqrt{\sigma_1})}{I_0(r_{ID}\sqrt{\sigma_1})}}{\frac{K_1(r_{ID}\sqrt{\sigma_1})}{I_1(r_{ID}\sqrt{\sigma_1})} + \frac{K_0(r_{ID}\sqrt{\sigma_1})}{I_0(r_{ID}\sqrt{\sigma_1})}} + \frac{zK_0(\sqrt{\sigma_1}) + \sqrt{\sigma_1}K_1(\sqrt{\sigma_1})}{I_0(r_{ID}\sqrt{\sigma_1})}} \quad (14)$$

$$\Delta_B = d_1(a_{23} - a_{33})$$

$$\sigma_2 = \frac{s D_1}{C_D e^{2S_1}}$$

2.3.2. Mathematical Model Solution – Second Stage

According to the diagnostic condition, if the following condition holds, the third stage gets involved.

$$\left(\bar{p}_{ID} \right)_{r_{ID}=r_{ID}} > \frac{1}{z} p_{PD} \quad (15)$$

2.3.3. Mathematical Model Solution – Third Stage

The mathematical model of the third stage is composed of equations (1), (2), (3), (4) and (7)-(10). The bottomhole pressure solution in the Laplace space is:

$$\bar{p}_{ID}(l, z) = \frac{\Delta_A I_0(\sqrt{\sigma_1}) + \Delta_B K_0(\sqrt{\sigma_1})}{\Delta} \quad (16)$$

Where,

$$a_{11} = zI_0(\sqrt{\sigma_1}) - \sqrt{\sigma_1}I_1(\sqrt{\sigma_1}); \quad a_{12} = zK_0(\sqrt{\sigma_1}) + \sqrt{\sigma_1}K_1(\sqrt{\sigma_1});$$

$$a_{13} = 0; \quad d_1 = \frac{1}{z}$$

$$a_{21} = 1; \quad a_{22} = -\frac{K_1(r_{ID}\sqrt{\sigma_1})}{I_1(r_{ID}\sqrt{\sigma_1})}; \quad a_{23} = \frac{\sqrt{\sigma_2/\sigma_1} K_1(r_{ID}\sqrt{\sigma_2})}{M I_1(r_{ID}\sqrt{\sigma_1})}; \quad d_2 = 0$$

$$a_{31} = 1; \quad a_{32} = \frac{K_0(r_{ID}\sqrt{\sigma_1})}{I_0(r_{ID}\sqrt{\sigma_1})};$$

$$a_{33} = -\left[\frac{K_0(r_{ID}\sqrt{\sigma_2})}{I_0(r_{ID}\sqrt{\sigma_1})} + S_2 r_{ID} \sqrt{\sigma_2} \frac{K_1(r_{ID}\sqrt{\sigma_2})}{I_0(r_{ID}\sqrt{\sigma_1})} \right]; \quad d_3 = 0$$

$$\Delta = a_{11}(a_{22}a_{33} - a_{23}a_{32}) + a_{12}(a_{23} - a_{33})$$

$$\Delta_A = d_1(a_{22}a_{33} - a_{23}a_{32})$$

3. WELL TEST CURVE FEATURES

3.1. Numerical Inversion

The Stehfest [15, 16] method is generally used for carrying out Laplace numerical inversion. This method is simple and easy to carry out, which produces results in very short time. It is used in this paper to achieve the numerical inversion on the bottom hole pressure in the Laplace space.

3.2. Type Curve Features

It can be seen from the log-log curve (Fig. 2 and Fig. 4) that there is obvious difference between the type curve which considers additional resistance on the interface and the conventional type curve. The curve can be divided into five stages:

- (1) Wellbore storage stage: The slope of pressure and pressure derivative curve is 1.0.
- (2) First transition stage: This stage is mainly controlled by wellbore storage and wellbore skin factor.
- (3) Infinite radial flow stage.
- (4) Second transition stage: This stage is mainly controlled by the interface parameters, including composite radius, breakout pressure difference (i.e. natural open fracture) and additional resistance. The composite radius controls the beginning time of the transition stage: the bigger the composite radius, the later the dynamic feature of the transition stage (Fig. 2). The breakout pressure difference affects the early pressure feature in this stage: the bigger the breakout pressure difference, the greater effect on pressure state, which may lead to minus pressure derivative (Fig. 3). The bigger the additional resistance skin factor (S_2), the

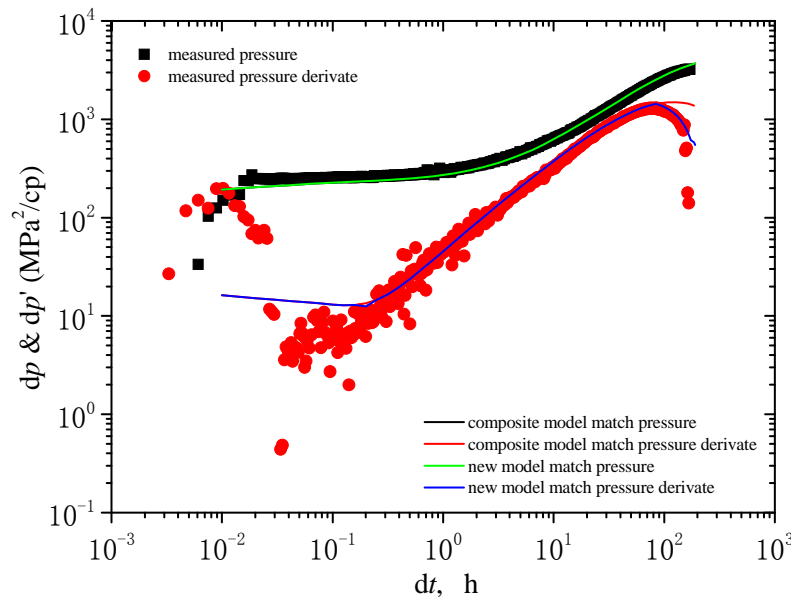


Fig. (5). Comparison of log-log match results of certain well

Table 1. Well test Interpretation Results in Certain Well

Model			Classic composite model	Composite model with additional resistance
Wellbore storage			m^3/MPa	0.1
Wellbore skin	S_1		dimensionless	1.5
Initial pressure			MPa	73.0
Formation factor			mD.m	1700
Permeability			mD	35.7
Composite parameters	Composite radius	r_1	m	130
	Flow coefficient ratio	M	dimensionless	150
	Storage parameter ratio	D_i	dimensionless	2.6
	Additional resistance skin	S_2	dimensionless	13.5

higher the pressure derivative height, which can override the effect of the breakout pressure difference (Fig. 4).

- (5) Second radial flow stage.
- (6) If the outer boundary is closed, then the derivative curve in the later time will be upwarping. It is the same as the conventional situation.

4. APPLICATION EXAMPLES

In the Tazhong 1 gas field, the effective thickness of producing interval in certain well is 47.6m, with a log interpretation porosity of 3.0%. Producing test lasted 207 days in this well. The total oil production is 5408.92 t, and the total gas production is $2288.79 \times 10^4 m^3$. Recharging feature occurred during producing process.

Based on the data of well test pressure and producing test pressure and flow rate, well test interpretation for its whole producing history was done. The log-log analysis result is shown in Fig. (5). There are 6 curves in Fig. (5). They are

the measured pressure and pressure derivate, match pressure and pressure derivate analyzed by composite model, match pressure and pressure derivate analyzed by the new model of this paper, respectively. It can be seen from Fig. (5) that the reservoir shows obvious composite gas reservoir features with poor properties in outer region, and the well test features and producing analysis are coincident; Moreover, the effect of parameters on interface are not considered in traditional models, thus its later fitting results were worse, while our model got better fitting results in the later stage.

The well test interpretation results are listed in Table 1. The major differences of the two models are in the following three parameters: mobility ratio, storage capacity ratio and additional resistance skin factor. The parameter M in the traditional model is up to 150, i.e., the outer zone permeability is only 0.24mD. Though its fitting result is good, it is contradictory to the stable producing feature during producing test period. The parameter M in the new model is 10, i.e., the outer zone permeability is 3.6mD.

Though its fitting result is good, it is contradictory to the stable producing feature during producing test period. Thus, it can provide enough energy for the inner zone which is coincident to geology features.

5. CONCLUSIONS

(1) Based on the analysis of production performance, a new well test model of effective well radius in composite reservoirs is set up. The open fracture and the additional resistance on interfaces are considered in this model, and log-log type curve is generated. The type curve can be divided into five stages. The emergence of the second transition stage is the major feature of this model. Some interface parameters (such as the composite radius, breakout pressure difference and additional resistance) affect the beginning time and curve form of the second transition stage.

(2) In our model, if we change the outer boundary conditions to closed circle boundary, then the type curves (such as Fetkovich and Blasingame, etc.) of some modern production analysis can be generated.

(3) For the well of Tazhong carbonate reservoir, whose abnormal composite model ($M > 100$, $D_i > 1$) shows the features of getting worse for the log-log curves in outer regions, it may reflect the well test features of composite with breakout pressure and additional resistance. This model can be diagnosed by combining modern production analysis.

(4) The major approach to reduce the ambiguity of interpretation is to describe the single well performance by combining data of short term buildup well test and long term production history, and by combining well test and modern production analysis. Dynamical description can solve key issues of single well or gas reservoir development, such as estimating reservoir permeability and evaluation stimulation, and it can also be used to analyze single well gas productivity, rate maintenance capability, dynamic reserve, interwell connectivity and water breakthrough.

CONFLICT OF INTEREST

The authors confirm that this article content has no conflicts of interest.

ACKNOWLEDGEMENTS

The author thanks the China Postdoctoral Science Foundation (No. 2011M500403 & No. 2012T50140) and Youth Foundation of China Petroleum Exploration and Development Research Institute (No. 2009-A-17-15) fund.

REFERENCES

- [1] Z. Xinyuan, W. Zhaoming, and Y. Haijun, "Cases of discovery and exploration of marine fields in China (Part 5): Tazhong Ordovician condensate field in Tarim basin", *Marine Origin Petroleum Geology*, vol. 11, no. 1, pp. 45-51, 2006.
- [2] Z. Xinyuan, L. Benliang, C. Zhuxin, Y. Hong-feng, and J. Bing, "The tectonic genesis and exploration targets of large oil-gas fields in Tazhong area, Tarim basin", *Xinjiang Petroleum Geology*, vol. 32, no. 3, pp. 211-217, 2011.
- [3] W. Zhaoming, Y. Haijun, and W. Zhenyu, *Characteristics of the Ordovician Carbonate in Tarim Basin*. Petroleum Industry Press: Beijing, 2010.
- [4] Z. Guangyou, Z. Shuichang, Z. Bin, S. Jin, and Y. Debin, "Reservoir types of marine carbonates and their accumulation model in western and central China", *Acta Petrolei Sinica*, vol. 31, no. 6, pp. 871-878, 2010.
- [5] S. Jin, Z. Shuichang, Y. Haijun, Z. Guangyou, C. Jianping, and Z. Bin, "Control of fault system to formation of effective carbonate reservoir and rules of petroleum accumulation", *Acta Petrolei Sinica*, vol. 31, no. 2, pp. 197-203, 2010.
- [6] S. Hedong, D. Xingliang, and S. Ying, "Characteristics of experimental project test and well test analysis of Tazhong No.1 gas fields", Tarim Oil Field Report, China: Petrochina, 2010, p. 4.
- [7] J.E. Junkin, M.A. Sippel, R.E. Collins, and M.E. Lord, "Well performance evidence for compartmented geometry of oil and gas reservoirs", In: *SPE Rocky Mountain Regional Meeting*, May 18-21, 1992, Casper, Wyoming, pp. 393-399, 1992.
- [8] L. Xinwei, "Well model of compound reservoir considering on additional resistance force on conjoining plate", *Petroleum Geology & Oilfield Development In Daqing*, vol. 20, no. 5, pp. 30-31, 2001.
- [9] W. Xiaodong, H. Xiaochun, and H. Mingqiang, "Pressure transient analysis in low-permeable media with threshold gradients", *Acta Petrolei Sinica*, vol. 32, no. 5, pp. 847-851, 2011.
- [10] C. Yuanqian, "Improper use of the starting pressure gradient of linear flow in the plane radial flow equation", *Acta Petrolei Sinica*, vol. 32, no. 5, pp. 847-851, 2011.
- [11] L.G. Acosta, and A.K. Ambastha, "Thermal well test analysis using an analytical multi-region composite reservoir model", In: *SPE Annual Technical Conference and Exhibition*, September 25-28, 1994, New Orleans, Louisiana, 1994, pp. 629-639.
- [12] W. Xingmei, Y. Sijun, and W. Jianwen, "Plane area reservoir well testing model including additional resistance", *Journal of Jiangnan Petroleum Institute*, vol. 25, no. S1, pp. 91-92, 2003.
- [13] L. Qiguo, F. Yu, and D. Fengling, "Study on testing interpretation model of dual medium and radial compound reservoir influenced by interface addition friction", *Well Testing*, vol. 14, no. 3, pp. 11-13, 2005.
- [14] L. Xiujun, L. Xiaoping, and L. Aimin, "Well test model of triple-medium complex reservoir considering interface friction", *Special Oil & Gas Reservoirs*, vol. 16, no. 3, pp. 74-76, 2009.
- [15] H. Stehfest, "Algorithm 368: Numerical inversion of Laplace transforms", *Communication of the ACM*, vol. 13, no. 1, pp. 47-49, 1970.
- [16] T. Dengke, and C Qinlei, "A note on Laplace numerical inversion of Stehfest method", *Acta Petrolei Sinica*, 2001, vol. 22, no. 6, pp. 91-92, 2001.

Received: September 20, 2012

Revised: January 07, 2013

Accepted: January 30, 2013

© He-Dong et al.; Licensee Bentham Open.

This is an open access article licensed under the terms of the Creative Commons Attribution Non-Commercial License (<http://creativecommons.org/licenses/by-nc/3.0/>) which permits unrestricted, non-commercial use, distribution and reproduction in any medium, provided the work is properly cited.